ISSN: 0973-3469, Vol.20, No.(1) 2023, Pg. 03-15

Material Science Research India

www.materialsciencejournal.org

Microstructure and Mechanical Properties of Functionally Graded AlSi/MWCNT Composite Cylinders

AZEEM PASHA* and B.M. RAJAPRAKASH

Department of Mechanical Engineering, UVCE, Bangalore University, Bangalore, Karnataka, India.

Abstract

Experimental fabrication of functionally graded Aluminum Silicon-carbon nanotubes (AlSi-MWCNT) reinforcement is significantly less, despite substantial theoretical interest. Many studies focused on axially layered functionally graded material because of ease of fabrication. Full advantage of AlSi-MWCNT functionally graded material only is taken when designed to the various shapes. In this research work, functionally graded cylinders were produced with 2wt% MWCNT at the outer surface to provide a complex and wear-resistant surface. The interior surface is soft with AlSi to provide elasticity. FGM1 sample indicates 112% and 11% increase in maximum tensile strength compared to AlSi and AlSi-MWCNT1wt%. FGM1 sample shows a 37% increase in elongation percentage compared to the AlSi-MWCNT1wt% composite. Test samples showing the typical nature of barrelling. FGM1 sample exhibits compressive strength of 237MPa, exceeding by 245% that of AlSi and by 3.5% that of AlSi-MWCNT1wt%. Three samples consider for each test. Hardness value ranges from 65HV at the core to 115HV at the outer surface. Hardness value Exceeds 56% in the outer layer compared to an inner region of FGM2.There is a proper bond between the layers, and the same demonstrate with properties of tensile, compressive, and hardness. OM with porosity, SEM with EDX evaluates to predict structural gradation in FGM cylinder.

Article History

Received: 11 January 2023

Accepted: 02 March 2023

Keywords

Aluminum Silicon (Alsi) Alloy; Functionally Graded Materials(Fgm); Multi Wall Carbon Nano Tubes (Mwcnt), Nano-Composites; Thermo-Mechanical Processing.

Introduction

Functionally graded materials are superior advanced materials with tailoring properties for the customer end product. Properties alter by controlling the constituent base matrix and reinforcement materials, which conventional alloys and composites are not possible. Tailoring properties makes them suitable for overcoming a wide variety of demanding problems such as thermal gradation, thermal mismatch, toughness, wear, corrosion, and impact.

CONTACT Azeem pasha sahabaazeem.786@gmail.com Department of Mechanical Engineering, UVCE, Bangalore University, Bangalore, Karnataka, India.

Doi: http://dx.doi.org/10.13005/msri/200102

The mechanical component wherein interior is soft and outer layer is tough, and wear-resistant benefitted from functionally graded material is shafts, gears, cams, and bearings. MWCNT reinforced nanofiller functionally graded materials are the trending newest materials investigated[1,2,3] Determines the FGM beams subjected longitudinal modeling. FEA modeling of axially functionally graded CNT Reinforced Composite.[4] Material topology of functionally graded beams subjected to bilateral constraints.[5] Studied instability of thermo-mechanical loaded graphene reinforced functionally graded materials. Young's modulus of graphene-FGM composite determined using modified Halpin–Tsai model.

[6]Functionally graded materials subjected to thermal shock resistance by considering (a) local tensile stress criterion, (b) thermal stress intensity factor criterion, and (c) hoop stress criterion.[7] Studies on Finite rotation multiple nodes (3 & 4) shell elements for functionally graded CNT-reinforced thin composite shells analysis. Reviewed FG-graphene reinforced *composite structures,* discuss mechanical properties, characteristics, and micro-mechanics model of FG-graphene composite.[6] carried out Fracture analysis of functionally graded material using extended element-free Galerkin method and digital image correlation technique; the experimental method helps fabricate a five-layered epoxy/glass FGM by hand layup process.

[9]Carried out Fracture analysis of functionally graded material using extended element-free Galerkin method and digital image correlation technique; the experimental method helps fabricate a five-layered epoxy/glass FGM by hand layup process.

[10]Fatigue behavior of FG-Ti–6Al–4V mesh structure fabricated by electron beam.[11] Reviewed mechanical properties of CNT reinforced functionally graded materials.[12] Carried out the analysis of wave propagation of CNT reinforced by FG- Composite cylindrical micro-shell using shear deformable shell theory and nonlocal strain gradient theory.[13] The modeling of functionally graded carbon nanotubes reinforced composite plates subjected to low-velocity impact with arbitrary geometry and general boundary conditions.[14] Studies on free vibration analysis and bending of FG-graphene vs CNT-reinforced composite plates.[15] Functionally graded-CNT cylindrical shell on dynamic buckling analyses of under axial power-law time-varying displacement load.1[6] Determines the temperature-dependent properties of functionally graded porous materials subjected to Thermoelastic analysis by a staggered finite volume method.[17] Functionally gradient brittle materials impact response characteristics and meso-evolution mechanism.[18] Three-dimensional flexural deformations of functionally graded material beams. Research carried out on functionally graded cylinders with radial gradation is significantly less; in this research work, the expensive CNT is provided on the surface to give hardness and strength. The interior remains soft to provide elasticity. The prepared material with geometry provides less cost, which offers powerful applications with lightweight, overall ductility, hard and wear-resistant surface desire: used in mechanical components of an automobile and aircraft.

Materials and Methods

Functionally graded cylinders fabricated by step by step procedure. The first step involves selecting materials such as atomized aluminum-silicon alloy powder with > 99% purity and Ni-coated MWCNTs (Hongwu Nanometer) and Aluminum silicon alloy powder constituents shown in Table.1 The average particle size of Aluminum silicon alloy powder is in the range of 50-70µm. Aluminum silicon alloy powder, ball-milled with Ni-coated MWCNTs having average diameters of 30-60nm and length of 1-2µm, the percentage of Nickel coated is <40% on MWCNTs in a Retsch PM-100 ball mill under argon atmosphere. Milling speed of 250rpm and 5:1 ball to powder weight ratio, milled for 5hours to avoid damage to Ni-coating and structure of the MWCNTs and acetone used to avoid cold welding of aluminum particles. Three composite concentrations prepare by dispersing 1wt%, 1.5wt%, and 2wt% MWCNT in the Aluminum silicon alloy powders. Two types of specimens fabricated one is Four-layer, and Two-layer sample prepare with an inner layer is milled Aluminum silicon alloy powder. The outer layer is Aluminum silicon alloy with MWCNTs variation (1, 1.5 & 2) weight percentage.

Figure. 1 sample considered FG2 where Centre milled AlSi will act as ductility layer, whereas MWCNTs wt% varied very marginally to avoid a

mismatch between layers. Three pieces fabricate to take the average of results. With a comparative test, AlSi-MWCNT nano-composites manufacture by same powder metallurgy route with varying MWCNT wt% by 1, 1.5 & 2.

Table 1: Composition of Aluminum silicon alloy powder.

Element	Composition (%)
Aluminum (Al)	85
Silicon (Si)	12.20
Magnesium (Mg)	1.0
Copper (Cu)	0.90
Nickel (Ni)	0.9

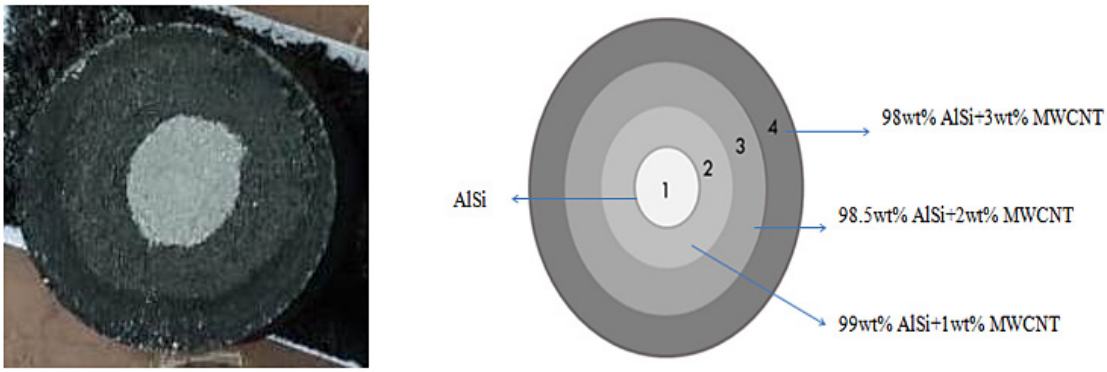

Fig. 1: Cross section of fabricated FGM sample showing4 layers of composition before hot extrusion.

Fabrication of FGM cylinders by a 16-part mold set is tedious and prone to damage to the layers of the FGM sample.[19]

3D mold spacer is a cylinder of length 75mm and outer diameter of 31mm. The internal pocket of a spacer divides with three pockets of diameter 23mm, 15mm, and 7mm separated with the minute thickness of 0.3mm. Each pocket provides three slots that aid in powder loading and rigidity to the mold. 3D mold spacer eliminates the use of lubricants, loading parts with mildew, and helps in avoiding contamination of the powders. The weighted percentages of each of the composition samples carefully pour using the small chimney. After filling, the mold is delicately removed from the cold compaction die to allow powders to fall in place and merge.

Figure 2. shows all the steps involved in the fabrication of the FGM cylinder. Cold compaction carries out using a KRYSTALTECH Universal Testing machine of capacity 600KN. Cold compacted FGM sample sintered at a temperature of 600oC for one h, then extruded with a ratio of 4:1.

It extruded samples machine for compression and Vickers micro-hardness test. For Compression and Tensile test, FGM1 sample used. Compression test conducted with ASTM E9-09 standard used for with L/D ratio of 1.5. Tensile specimen of diameter 15mm and 32-gauge length.

For the Compression test, the compaction rate of 0.5mm/min is fixed and continued until a maximum strain of 50%—three samples of each composition prepared.

Optical microscopy characterizes each layer's microstructure of FGM and data collection from Nikon Microscope LV150 with Clemex Image

Analyser. A porosity test determines the size of the pores to evaluate the proper densification of each layer in the FGM sample. SEM (TESCAN-VEGA3 LMU) analyzes the Ni-coated MWCNT dispersion in the Aluminum silicon alloy matrix operating at 15 kV and 20nA. Compositional characteristics determine by EDX. XRD (X-Ray Diffraction Analyzer) 30 mA, 45 kV peaks to analyze the crystal structure orientations with element presence and data collection software is X'Pert Data Collector.

Fig. 2: shows all the steps involved in fabrication of FGM cylinder by powder metallurgy.

Results and Discussion

Powder Characterization

SEM images of AlSi, AlSi-1wt%MWCNT, AlSi-1.5wt%MWCNT and AlSi-2wt%MWCNT composite milled powders shown in Fig.4 (a-d) are showing typical morphology of powders.

They are coarsening of particles due to cold welding in the ball milling process, clearly seen in Figure.3(a-d). SEM analysis indicates the uniform dispersion of MWCNTs in Aluminum silicon alloy particles, and in some parts, there is an agglomeration of bonded particles. AlSi-MWCNT particles showing irregular morphology and rough surfaces compared to AlSi. SEM images prove the effectiveness of ball milling parameters (Ball milling time, speed, BPR & PCA amounts) used in this research helps avoid MWCNT clusters.[20] The particle size, morphology, and composition of constituents influence the compaction and sintering of FGM cylinders, mainly helps in interfacial strength between the layers.

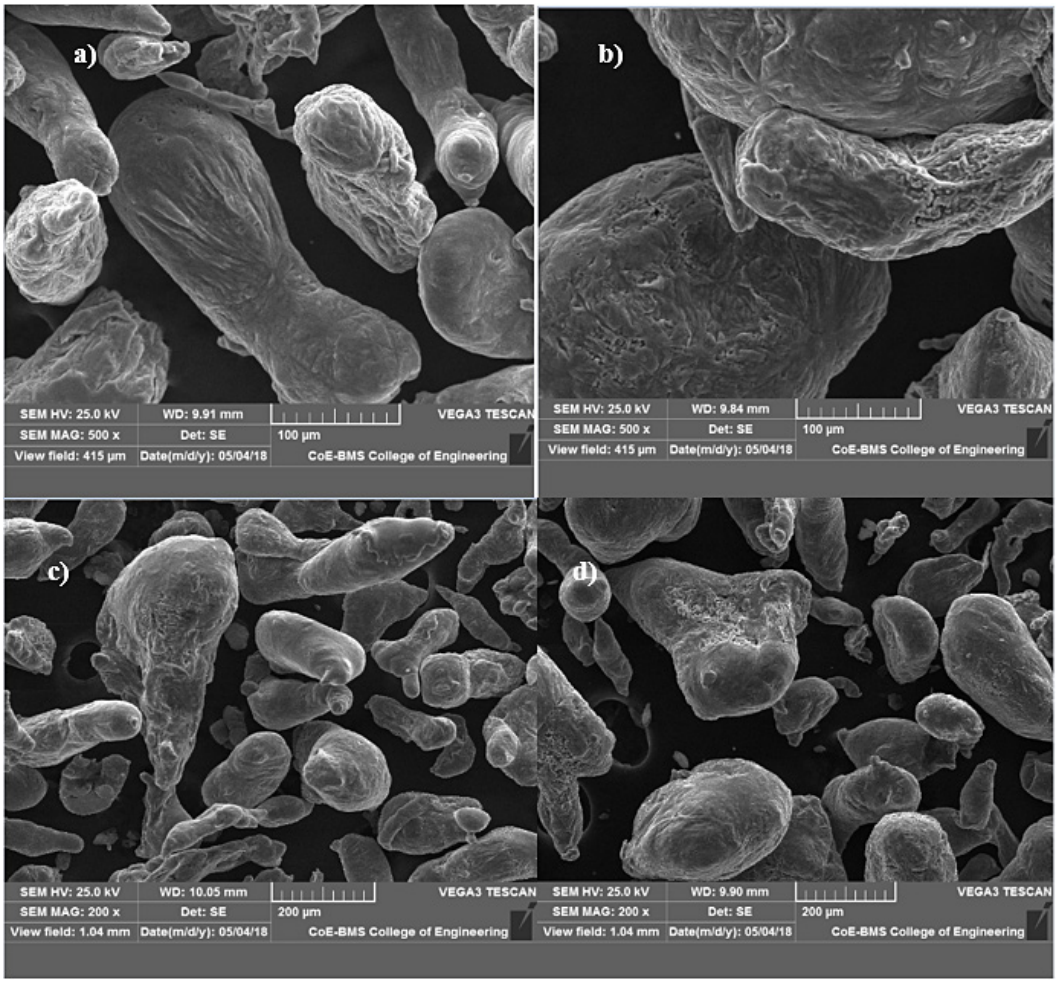

Fig. 3: SEM showing typical morphology of the a) AlSi, b) AlSi-1wt%MWCNT, c) AlSi-1.5wt%MWCNT and d) AlSi-2wt%MWCNT composite milled powders.

Optical Microscopy and Porosity

Optical microscopy of FGM sample with an inner layer is AlSi, and the outer layer is AlSi-MWCNT, there is no presence of crack between each layer as discussed by,[20] didn't occur in this research. The microstructure consists of uniformly dispersed eutectic silicon particles. Intermetallic phases in the inter-dendritic region in the matrix of aluminum solid solution. (~5-8%) Porosity observed in sample Fig.4(a). the layer of AlSi-1.5wt%MWCNT porosity reduces to 5% shown in Fig.4(b) and AlSi-2wt%MWCNT limited to 3% in Fig.4(c), it is a positive sign of good compaction and sintering. Uniform dispersion of multiwall carbon nanotubes (MWCNT) in AlSi matrix helps in reducing the porosity to an extent of weight percentage of 2wt%.[21-23]

SEM analysis with EDX of FGM cylinders

Sample No 1, AlSi + (1wt % Ni-MWCNT +AlSi)

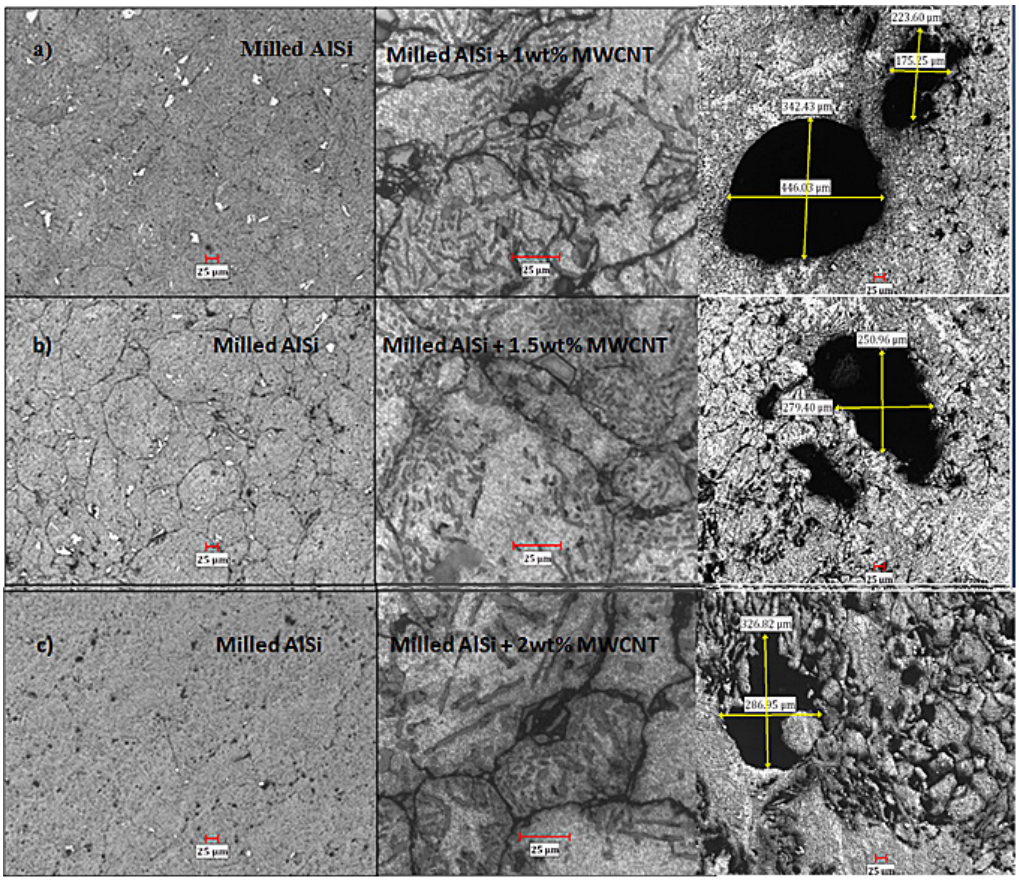

Fig. 4: (a-c) shows optical microscopy of FGM1 cylinder with respect to layers and Porosity in each layer.

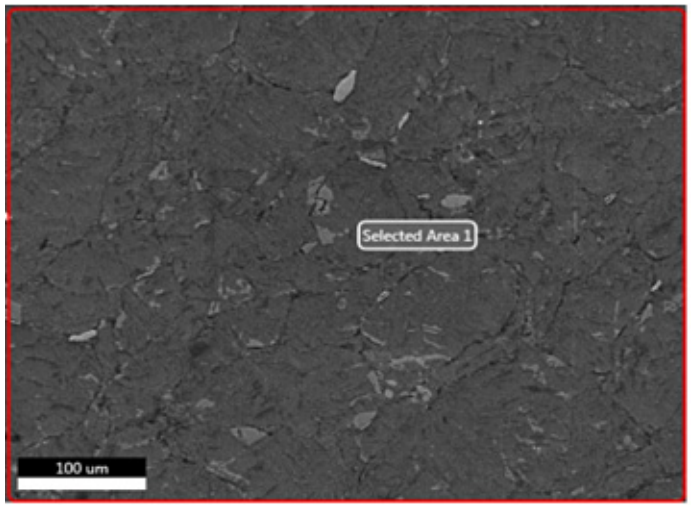

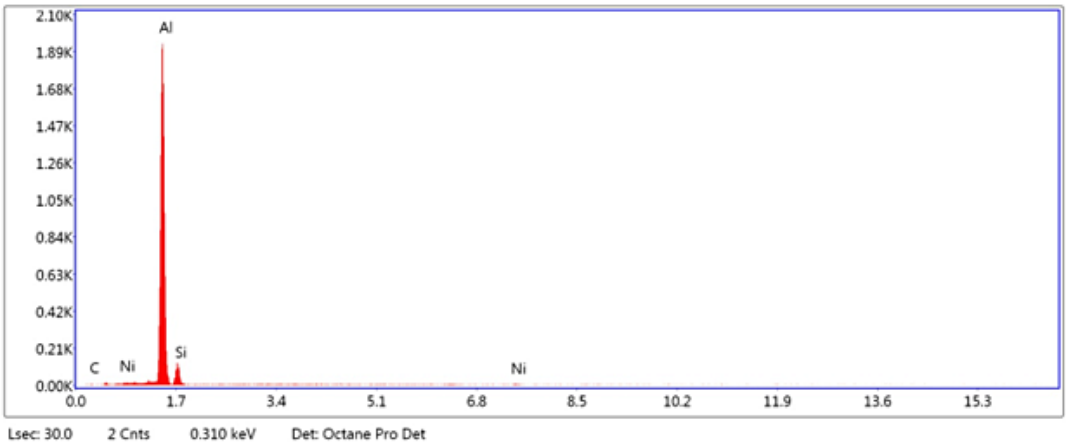

Element	Weight %	Atomic %
C K	4.62	9.89
AlK	76.99	73.42
SiK	18.07	16.55
NiK	0.33	0.14

Sample No 2, AlSi + (1.5wt % Ni-MWCNT +AlSi)

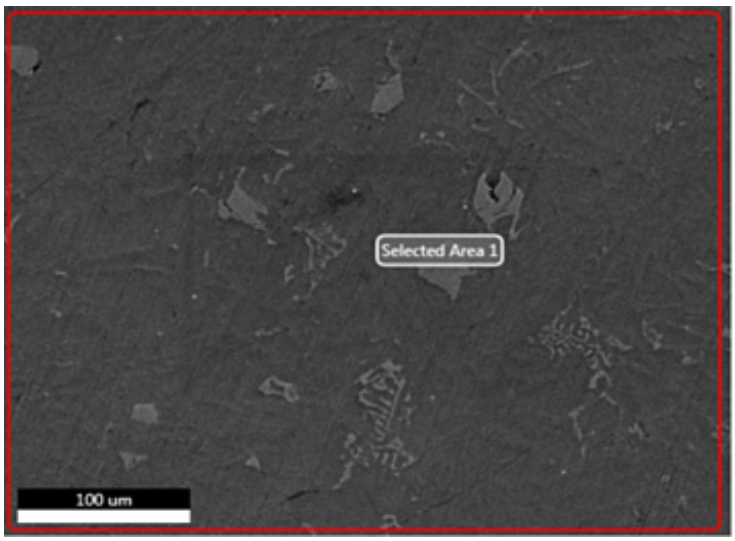

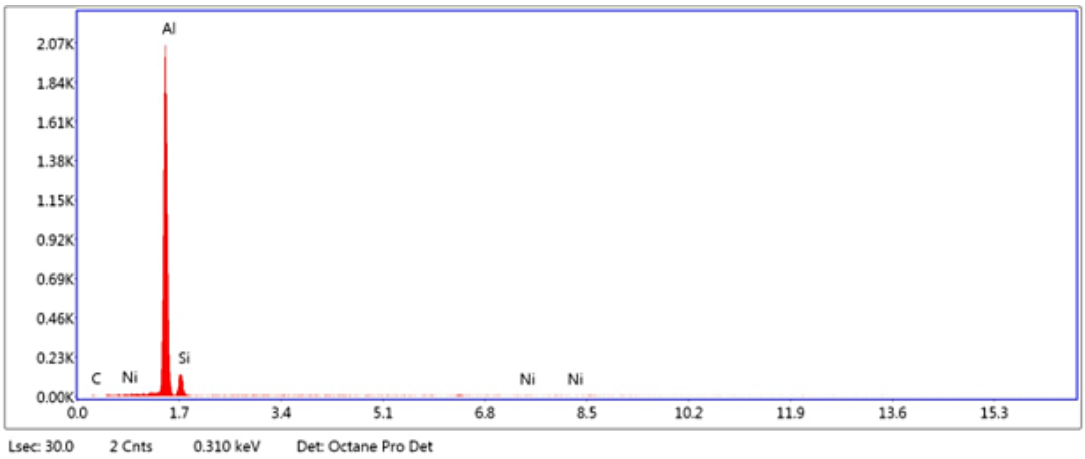

Element	Weight %	Atomic %
C K	4.83	10.34
AlK	77.14	73.48
SiK	17.37	15.89
NiK	0.65	0.29

Sample No 3, AlSi + (2wt % Ni-MWCNT +AlSi

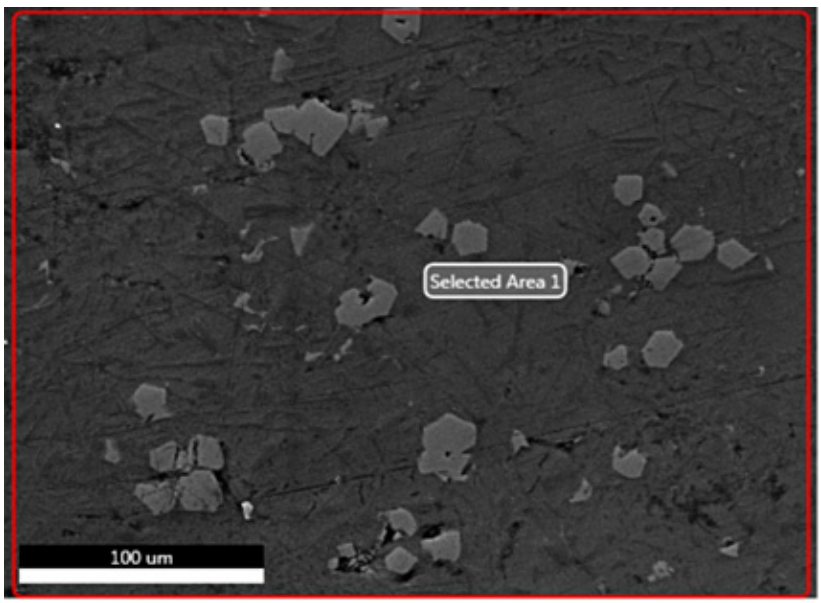

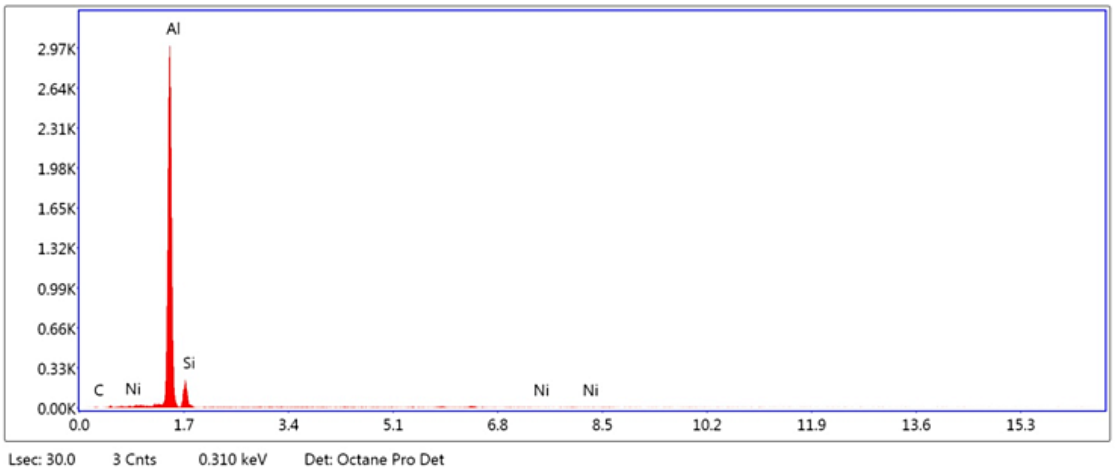

Element	Weight %	Atomic %
C K	5.37	11.42
AlK	78.50	74.37
SiK	15.12	13.76
NiK	1.01	0.44

Fig. 5: (a-c) shows SEM with EDX (a) AlSi-Ni-MWCNT1wt%, (a) AlSi-Ni-MWCNT1.5wt%, & (a) AlSi-Ni-MWCNT2wt%.

SEM images with EDX of AlSi with Ni coated MWCNT are seen in Figure.5 (a-c). SEM images indicating the uniform dispersion of MWCNTs in the Aluminum silicon alloy matrix with Ni content presence in EDX graph, and the same thing proved with weight percentage. Ni coating on MWCNTs helps improve the dispersion in the AlSi matrix. Proper uniform distribution helps enhance the properties of the FGM material, and the same is portray in tensile and compressive properties.

Mechanical Properties

The tensile test evaluates the mechanical behavior of FGM samples. Challenge occurs during machining of FGM sample to reduce cross-section. It will remove the outer part of the FGM layer, which consists of a higher concentration of MWCNT it would affect mechanical properties. FGM machined to the ASTM standard as shown in Figure.8 it is possible to reduce it to 14.5mm diameter, and grips, on the other hand, is 16mm as same been followed in.[19] FGM1 samples fracture to the middle of the gauge length. FGM1 sample fracture by the combined effect of ductile and brittle nature.

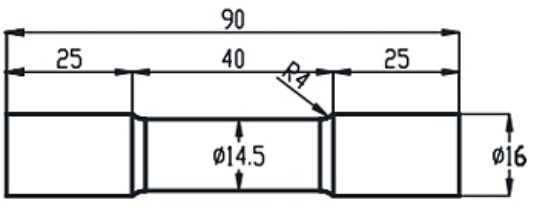

Fig. 6: FGM machined sample for tensile test

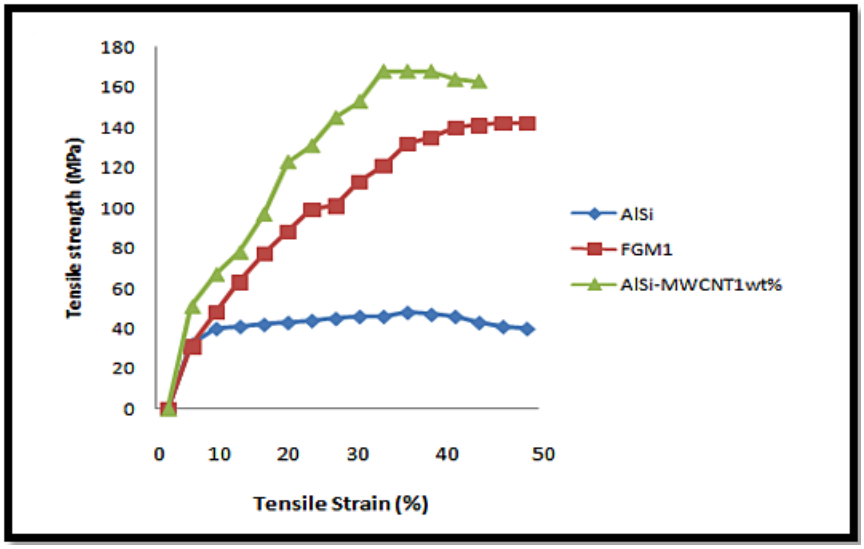

Fig. 7: shows tensile stress and strain diagram for AlSi, FGM1 and AlSi-MWCNT1wt%

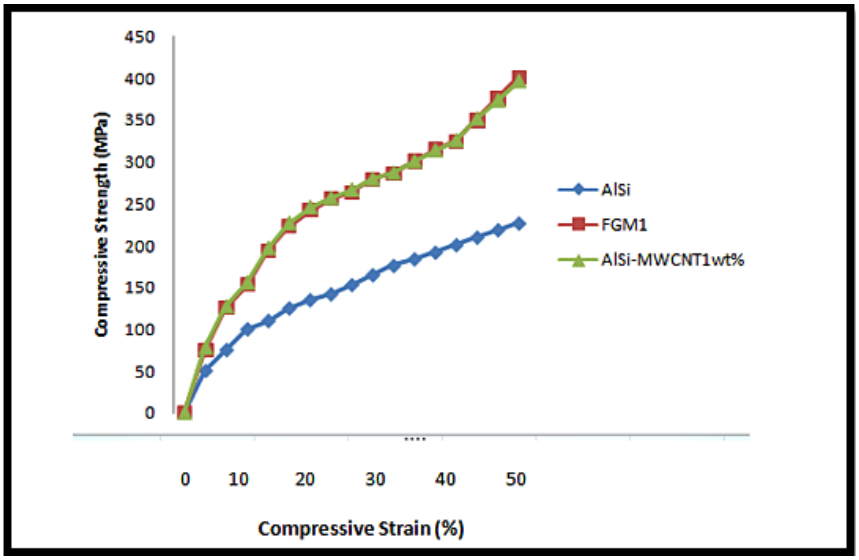

Fig. 8: shows Compressive stress and strain diagram for AlSi, FGM1 and AlSi-MWCNT1wt%

Figure 7. shows the Stress-strain diagram of tensile behavior of AlSi, AlSi-1wt%MWCNT, and FGM1. AlSi-MWCNT1wt% and FGM1 exhibit an increase in ultimate tensile strength compared to AlSi. FGM1 sample indicates 112% and 11% increase in maximum tensile strength compared to AlSi and AlSi-MWCNT1wt%. FGM1 sample shows a 37% increase in elongation percentage compared to the AlSi-MWCNT1wt% composite.

FGM1 sample exhibits lower yield strength of 57Mpa compared 96Mpa for AlSi-1wt%MWCNT composite. Low yield strength of FGM1 due to milled AlSi ductile nature in layer1.

Figure. 8 represents the Compressive stress-strain diagram for AlSi, FGM1, and AlSi-MWCNT1wt%. No breaking or fracturing of layers until machine strain rate reaches 50% hence confirms strong

bond between the layers. There is no delamination of layers. Test samples showing the typical nature of barrelling. FGM1 sample exhibits compressive strength of 237MPa, exceeding by 245% that of AlSi and by 3.5% that of AlSi-MWCNT1wt%. Three samples consider for each test.

Vicker's hardness test conducts on FGM2 with four layers to capture at the interface between layers. Figure.9 shows hardness values in the FGM2 sample from the center to the outer surface. Average values of 20-25 readings of hardness taken in each region. Hardness values increase from the center to the outer region. Hardness value ranges from 65HV at the core to 115HV at the outer surface. Hardness value Exceeds 56% in the outer layer compared to an inner region of FGM2.

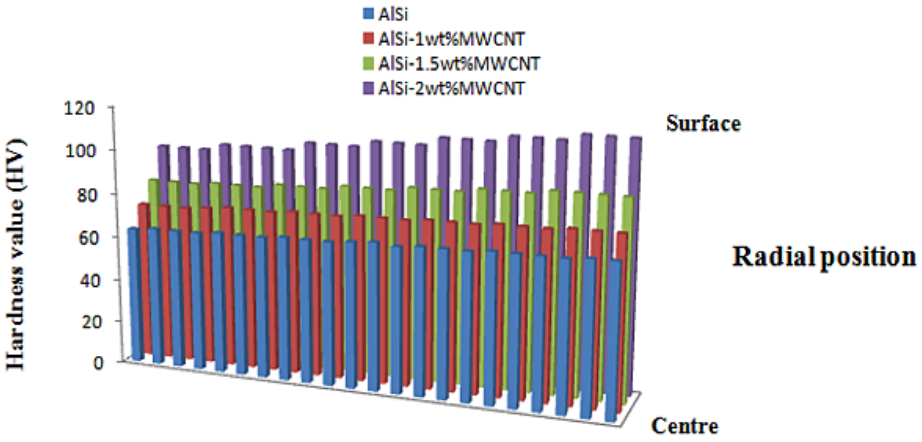

Fig. 9: Vicker's hardness values for FGM2 with respect to radial direction from Centre to outer surface.

Conclusion

Research carried out on FGM cylinder is very little. Only axially layered FGMs were fabricated due to processing constraints. Theoretical studies indicate various shapes of FGM are fabricated such as conical shapes, panels, beams, discs, cylinders and plates. Present work demonstrates the FGM cylinders with radial CNT composition gradient.

Tensile test results predict FGM performs well compared to base AlSi, and AlSi-1wt%MWCNT provides a better combination between strength and ductility. Micro-Vickers hardness value indicates the outer surface is more hard compared to the core. The compressive properties of FGM cylinders provide more stability and sustainability compared to base AlSi and AlSi-1wt%MWCNT. Micro structural evaluation carries out with Optical microscopy with porosity, and SEM with EDX provides structural gradation of FGM layers.

The produced FGM cylinders provide the solution to a wide variety of challenges of drive shaft designs. It will provide toughness, strength, and lightweight.

Acknowledgement

Authors would like to thank Principal of constituent college for continuous support and encouragement.

Funding

There is no funding for this research work.

Conflict of Interest

There is no conflict of interest among authors.

References

1. H. Salavati *et al.,* 'Titanium/Zirconium functionally graded materials with porosity gradients for potential biomedical applications', Geophysical Research Letters, vol. 36, no. 1, pp. 972–977, 2020, doi: 10.1016/j.compositesb.2018.11.076.
2. R. M. Mahamood and E. T. Akinlabi, 'Laser metal deposition of functionally graded Ti6Al4V/TiC', *Materials and Design,* vol. 84, pp. 402–410, Nov. 2015, doi: 10.1016/j.matdes.2015.06.135.
3. A. M. El-Ashmawy and Y. Xu, 'Longitudinal modeling and properties tailoring of functionally graded carbon nanotube reinforced composite beams: A novel approach', *Applied Mathematical Modelling,* vol. 88, pp. 161–174, 2020, doi: 10.1016/j.apm.2020.06.043.
4. T. Salem, P. Jiao, I. Zaabar, X. Li, R. Zhu, and N. Lajnef, 'Functionally Graded Materials Beams Subjected to Bilateral Constraints: Structural Instability and Material Topology', *International Journal of Mechanical Sciences,* vol. 194, no. November 2020, p. 106218, 2021, doi: 10.1016/j.ijmecsci.2020.106218.
5. H. Wu, J. Yang, and S. Kitipornchai, 'Parametric instability of thermo-mechanically loaded functionally graded graphene reinforced nanocomposite plates', *International Journal of Mechanical Sciences,* vol. 135, no. November 2017, pp. 431–440, 2018, doi: 10.1016/j.ijmecsci.2017.11.039.
6. Y. Zhang, L. Guo, X. Wang, R. Shen, and K. Huang, 'Thermal shock resistance of functionally graded materials with mixed-mode cracks', *International Journal of Solids and Structures,* vol. 164, pp. 202–211, 2019, doi: 10.1016/j.ijsolstr.2019.01.012.
7. A. Frikha, S. Zghal, and F. Dammak, 'Finite rotation three and four nodes shell elements for functionally graded carbon nanotubes-reinforced thin composite shells analysis', *Computer Methods in Applied Mechanics and Engineering,* vol. 329, pp. 289–311, 2018, doi: 10.1016/j.cma.2017.10.013.
8. S. Zhao, Z. Zhao, Z. Yang, L. L. Ke, S. Kitipornchai, and J. Yang, 'Functionally graded graphene reinforced composite structures: A review', *Engineering Structures,* vol. 210, no. January, p. 110339, 2020, doi: 10.1016/j.engstruct.2020.110339.
9. W. Farouq, H. Khazal, and A. K. F. Hassan, 'Fracture analysis of functionally graded material using digital image correlation technique and extended element-free Galerkin method', *Optics and Lasers in Engineering,* vol. 121, no. November 2018, pp. 307–322, 2019, doi: 10.1016/j.optlaseng.2019.04.021.
10. Q. S. Wang *et al.,* 'Mechanistic understanding of compression-compression fatigue behavior of functionally graded Ti–6Al–4V mesh structure fabricated by electron beam melting', *Journal of the Mechanical Behavior of Biomedical Materials,* vol. 103, no. December 2019, 2020, doi: 10.1016/j.jmbbm.2019.103590.
11. K. M. Liew, Z. X. Lei, and L. W. Zhang, 'Mechanical analysis of functionally graded carbon nanotube reinforced composites: A review', *Composite Structures,* vol. 120, pp. 90–97, 2015, doi: 10.1016/j.compstruct.2014.09.041.
12. H. Zeighampour and Y. T. Beni, 'Size dependent analysis of wave propagation in functionally graded composite cylindrical microshell reinforced by carbon nanotube', *Composite Structures,* vol. 179, pp. 124–131, 2017, doi: 10.1016/j.compstruct.2017.07.071.
13. M. Fallah, A. R. Daneshmehr, H. Zarei, H. Bisadi, and G. Minak, 'Low velocity impact modeling of functionally graded carbon nanotube reinforced composite (FG-CNTRC) plates with arbitrary geometry and general boundary conditions', *Composite Structures,* vol. 187, no. September 2017, pp. 554–565, 2018, doi: 10.1016/j.compstruct.2017.11.030.
14. E. García-Macías, L. Rodríguez-Tembleque, and A. Sáez, 'Bending and free vibration analysis of functionally graded graphene vs. carbon nanotube reinforced composite plates', *Composite Structures,* vol. 186, no. December 2017, pp. 123–138, 2018, doi: 10.1016/j.compstruct.2017.11.076.

15. P. Jiao, Z. Chen, Y. Li, H. Ma, and J. Wu, 'Dynamic buckling analyses of functionally graded carbon nanotubes reinforced composite (FG-CNTRC) cylindrical shell under axial power-law time-varying displacement load', *Composite Structures,* vol. 220, no. April, pp. 784–797, 2019, doi: 10.1016/j.compstruct.2019.04.048.
16. J. Gong, L. Xuan, B. Ying, and H. Wang, 'Thermoelastic analysis of functionally graded porous materials with temperature-dependent properties by a staggered finite volume method', *Composite Structures,* vol. 224, no. 947, p. 111071, 2019, doi: 10.1016/j.compstruct.2019.111071.
17. Y. Li, T. Wang, and M. Zhou, 'Impact response characteristics and meso-evolution mechanism of functionally gradient brittle materials with pore hole damage', *Composite Structures,* vol. 256, no. June 2020, p. 112989, 2021, doi: 10.1016/j.compstruct.2020.112989.
18. R. C. Batra, 'Material tailoring in three-dimensional flexural deformations of functionally graded material beams', *Composite Structures,* vol. 259, no. October 2020, p. 113232, 2021, doi: 10.1016/j.compstruct.2020.113232.
19. E. I. Salama, S. S. Morad, and A. M. K. Esawi, 'Fabrication and mechanical properties of aluminum-carbon nanotube functionally-graded cylinders', *Materialia,* vol. 7, no. May, p. 100351, 2019, doi: 10.1016/j.mtla.2019.100351.
20. A. *et al*. AzeemPasha *et al.,* 'Hardness And Microstructure Of Functionally Graded Aluminium Silicon Alloy With Multiwall Carbon Nanotube Composite By Powder Metallurgy With Hot Extrusion Technique', International Journal of Mechanical and Production Engineering Research and Development, vol. 10, no. 3, pp. 12279–12288, 2020, doi: 10.24247/ijmperdjun20201174.
21. Azeem Pasha and B.M Rajaprakash, "Functionally graded materials (FGM) fabrication and its potential challenges & applications," *Materials Today: Proceedings*, Volume 52, part 3, Pages 413-418, (2022).
22. Azeem Pasha and B.M Rajaprakash, "Effect of CNT content on microstructure and hardness of AlSi/MWCNT nano composite", *Materials Today: Proceedings,* Volume 49, part5, Pages 1345-1350, (2022).
23. Azeem Pasha and B.M Rajaprakash, "Fabrication and mechanical properties of functionally graded materials: A review," *Materials Today: Proceedings,* Volume 52, part 3, Pages 379-387, (2022).